Journal of Materials Chemistry C

Accepted Manuscript

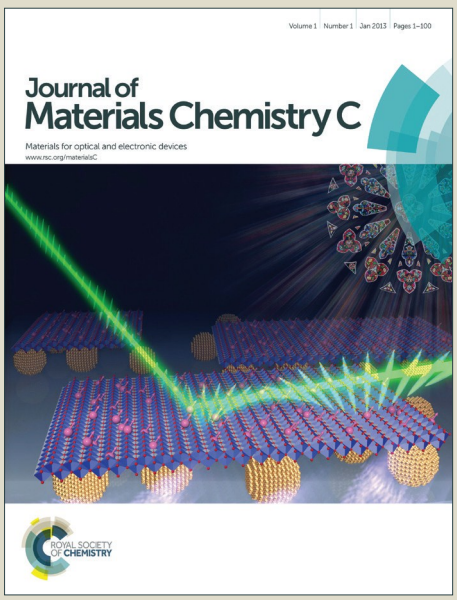

This is an *Accepted Manuscript*, which has been through the Royal Society of Chemistry peer review process and has been accepted for publication.

Accepted Manuscripts are published online shortly after acceptance, before technical editing, formatting and proof reading. Using this free service, authors can make their results available to the community, in citable form, before we publish the edited article. We will replace this *Accepted Manuscript* with the edited and formatted *Advance Article* as soon as it is available.

You can find more information about *Accepted Manuscripts* in the Information for Authors.

Please note that technical editing may introduce minor changes to the text and/or graphics, which may alter content. The journal's standard Terms & Conditions and the Ethical guidelines still apply. In no event shall the Royal Society of Chemistry be held responsible for any errors or omissions in this *Accepted Manuscript* or any consequences arising from the use of any information it contains.

ROYAL SOCIETY OF CHEMISTRY

www.rsc.org/materialsC

$PbGa_4S_7$: A Wide-Gap Nonlinear Optical Material†

Xiaoshuang Li,[abc] Lei Kang,[abc] Chao Li,[abc] Zheshuai Lin,[ab] Jiyong Yao,*[ab] and Yicheng Wu[ab]

By combining the [GaS_4] tetrahedra and the second-order Jahn–Teller distorted cation Pb^{2+}, a new wide-gap nonlinear optical material $PbGa_4S_7$ has been obtained. In the structure, Pb^{2+} is coordinated to a distorted quadrangular pyramid of five S atoms, showing the stereo-chemical activity of the $6s^2$ lone pair electron. The polar arrangement of the [GaS_4] tetrahedra and the macroscopic arrangement of the [PbS_5] distorted quadrangular pyramids result in a large IR nonlinear optical property for $PbGa_4S_7$, which is ~1.2 times that of the benchmark $AgGaS_2$ at a laser radiation of 2.09 μm. Moreover, $PbGa_4S_7$ has a large direct band gap of 3.08(2) eV, a desirable property for avoiding two-photon absorption of the conventional 1~2 μm pumping laser sources and improving the laser damage threshold. The DSC analysis indicates that the compound is thermally stable up to 1140 K. The electronic structure was also calculated to explain the optical properties.

[a] *Center for Crystal Research and Development, Technical Institute of Physics and Chemistry, Chinese Academy of Sciences, Beijing 100190, P.R. China, Email: jyao@mail.ipc.ac.cn*

[b] *Key Laboratory of Functional Crystals and Laser Technology, Chinese Academy of Sciences, Beijing 100190, P.R. China*

[c] *University of Chinese Academy of Sciences, Beijing 100049, P.R. China*

†Electronic supplementary information (ESI) available: Crystallographic data in CIF format for $PbGa_4S_7$.

Journal of Materials Chemistry C Accepted Manuscript

Introduction

Infrared (IR) coherent laser sources, especially those covering the two important atmospheric transparent windows (3−5 and 8−12 μm), are of great application value in military and civil fields, such as laser guidance, atmospheric laser communications, environmental monitoring, noninvasive medical diagnostics, etc.[1−4] IR nonlinear optical (NLO) crystals are an important class of crystals to realize the output of such lasers through frequency conversion of the near IR lasers.[5] However, to date, only a few IR NLO crystals are commercially available—$AgGaS_2$,[6,7] $AgGaSe_2$,[8,9] and $ZnGeP_2$.[10] Unfortunately, each of them suffers from drawbacks that severely limit their wider application — for example, $AgGaQ_2$ (Q = S, Se) has a low laser-damage threshold, $AgGaSe_2$ can not achieve phase matching at ~1 μm, and $ZnGeP_2$ exhibits strong two-photon absorption of the conventional 1~2 μm pumping laser. Hence, the exploration for new IR NLO materials with better overall properties is extremely urgent.

During the last decades, researches were widely carried out on metal chalcogenides,[11-15] which is a rich source of nonlinear optical materials,[16] leading to the discovery of many new materials with attractive IR NLO properties, such as $BaGa_4Q_7$ (Q = S, Se),[17,18] $Li_2In_2MQ_6$ (M = Si, Ge; Q = S, Se),[19] $BaGa_2MQ_6$ (M = Si, Ge; Q = S, Se),[20] $Pb_4Ga_4GeQ_{12}$ (Q = S, Se),[21] and $Ba_{23}Ga_8Sb_2S_{38}$,[22] which possess large NLO responses that mainly originate from distorted [MQ_4] (M = In, Ga, Si, Ge; Q = S, Se) tetrahedra. At the same time, other compounds, including $SnGa_4Q_7$ (Q = S, Se),[23] $AZrPSe_6$(A = K, Rb, Cs)$_8$,[24] $AAsQ_2$ (A = Li, Na; Q = S, Se),[25] $A_3Ta_2AsS_{11}$ (A =

Journal of Materials Chemistry C Accepted Manuscript

K, Rb),[26] were also reported to exhibit very strong NLO responses in middle IR. These compounds demonstrated that the second-order Jahn–Teller (SOJT) distorted cations, such as d^0 transition metal ions (e.g., Ta^{5+},Zr^{4+}), d^{10} cations with large polar displacement, and p-block cations with stereochemically active lone-pair electrons (e.g., Pb^{2+}, Bi^{3+}, IO^{3-}), can also contribute to second harmonic generation (SHG) properties as a result of the "additive" effect of these types of polarization groups.[27-35] Similar phenomena were observed in the UV NLO borates $Cd_4BiO(BO_3)_3$,[36] and $BaNbO(IO_3)_5$[37] as well.

These research results stimulate our interest in A-Ga-Q (Q = S, Se, Te) system in which A refers to cations with lone pair electrons, in particular, Bi or Pb, hoping to achieve large NLO responses through combining the [GaQ_4] tetrahedra and the SOJT distorted Pb^{2+} or Bi^{3+} cations. Currently, only a few ternary compounds are known in these systems: including the Pb-Ga-Q (Q = S, Se, Te) compounds $Pb_2Ga_2S_5$,[38] $PbGa_2Se_4$,[39] $PbGa_6Te_{10}$,[40] and the Bi-Ga-Q (Q = S, Se, Te) compounds $Bi_2Ga_4Q_8$ (Q = S, Se),[41] none of which were reported to exhibit NLO properties. In this work, we discovered one new ternary noncentrosymmetric (NCS) compound — $PbGa_4S_7$. It exhibits a large powder SHG response that is ~ 1.2 times that of benchmark $AgGaS_2$ at a laser radiation of 2.09 μm. The origin of SHG response and the characteristics of lone pair electrons on Pb^{2+} cation are discussed. Moreover, it possesses a large band gap of about 3.08 eV, a property desirable for increasing the laser damage threshold and avoiding the two-photon absorption of the conventional 1~2 μm pumping laser sources.

Journal of Materials Chemistry C Accepted Manuscript

Experimental section

Reagents.

The following reagents were used as obtained: Pb (Sinopharm Chemical Reagent Co., Ltd., 99.9%), Ga (Sinopharm Chemical Reagent Co., Ltd., 99.99%), Bi (Sinopharm Chemical Reagent Co., Ltd., 99.99%), and S (Sinopharm Chemical Reagent Co., Ltd., 99.9999%). The binary starting materials, PbS, Ga_2S_3, and Bi_2S_3 were synthesized by the stoichiometric reactions of elements at high temperatures (1023 K for PbS, 1273 K for Ga_2S_3, and 573 K for Bi_2S_3) in sealed silica tubes evacuated to 10^{-3} Pa.

Synthesis of $PbGa_4S_7$.

Numerous attempts, including adjusting the composition of the starting materials, changing the reaction temperatures and introducing flux, were made to obtain new NCS compounds in Pb-Ga-Q (Q = S, Se, Te) system. Attempts by adjusting composition of starting materials or temperatures failed to discover new NCS compounds, but the use of the Bi_2S_3 flux led to the discovery of the $PbGa_4S_7$ compound.

In the first approach, the mixtures of PbQ (Q = S, Se, Te) and Ga_2Q_3 in several molar ratios ranging from 3:1 to 1:3 were ground and loaded into fused-silica tubes under an Ar atmosphere in a glovebox,. The tubes were flame sealed under a high vacuum of 10^{-3} Pa and then placed in a computer-controlled furnace. The samples were heated to different temperatures ranging from to 1173 K to 1323 K in 24 h and kept at that temperature for 96 h, then cooled at a slow rate of 3 K/h to 623 K, and

Journal of Materials Chemistry C Accepted Manuscript

finally cooled to room temperature naturally. Yellow and red crystals were obtained, which were stable in air for months. But analyses of the crystals with an EDX-equipped Hitachi S-4800 SEM and single crystal X-ray diffraction revealed the previously reported $PbGa_2Q_4$ (Q = S, Se) and $PbGa_6Te_{10}$ as a major product in all these reactions and trace of $PbGa_6Q_{10}$ (Q = S, Se) with poor quality at 1323 K.

In the second approach, inspired by the facts that a series of arsenides and germanides, including $LaCo_2As_2$,[42] $Ln_2Fe_4Sb_5$,[43] Ce_2CuGe_6,[44] and $LnCoGe_3$ (Ln = Ce, Pr, Nd),[45] could be synthesized in Bi flux, we tried Bi_2Q_3 (Q = S, Se) as flux in the reaction between PbQ and Ga_2Q_3. In a typical reaction, powders of PbQ, Ga_2Q_3, and Bi_2Q_3 were mixed in the 1:2:1 ratio, and then sealed in fused-silica tubes under an Ar atmosphere in a glovebox. The samples were heated to 1273 K in 24 h and kept at 1273 K for 48 h, then cooled at a slow rate of 3 K/h to 623 K, and finally cooled to room temperature naturally. Yellow crystals were obtained, which were hand-picked from the melts for analysis. The yields were about 50% based on Pb. Elemental analyses confirmed the appearance of Pb, Ga, and Q in the approximate ratio of 1:4:7 for the reactions and no bismuth was detected in the crystals. However, the selenide product is still not good enough for structure determination after many attempts. The yellow sulfide product $PbGa_4S_7$ is of good quality and stable in the air for weeks.

Structure Determination.

Single-crystal X-ray diffraction data of $PbGa_4S_7$ were collected with the use of graphite-monochromatized Mo Kα (λ = 0.71073 Å) at 153 K on a Rigaku AFC10

Journal of Materials Chemistry C Accepted Manuscript

diffractometer equipped with a Saturn CCD detector. Crystal decay was monitored by re-collecting 50 initial frames at the end of data collection. The collection of the intensity data, cell refinement and data reduction was carried out with the use of the program Crystalclear.[46] Face-indexed absorption corrections were performed numerically with the use of the program XPREP.[47]

The structure was solved with the direct methods program SHELXS and refined with the least-squares program SHELXL of the SHELXTL.PC suite of programs.[47] The final refinement included anisotropic displacement parameters and a secondary extinction correction. Additional experimental details are given in Table 1 and selected metrical data are given in Table 2. Further information may be found in the supplementary information.

Powder X-ray Diffraction.

Single crystals of $PbGa_4S_7$ (about 0.3 g) were hand-picked from reaction products and ground to powder. Then the powder X-ray diffraction (PXRD) patterns of the ground powder before and after melting were collected on a Rigaku MiniFlex II diffractometer (Cu Kα radiation, λ = 1.5406 Å) at 153 K. The 2θ range is 10−70 °, with a step size of 0.02 ° and a scan speed of 0.1 s/step. PXRD pattern before melting is in good agreement with the simulated patterns generated using the CIF of the refined structure, proving the purity of the bulk sample, while the pattern after melting is not (see Fig. 1). This phenomenon will be discussed in the thermal analysis section.

Thermal Analysis.

Journal of Materials Chemistry C Accepted Manuscript

A Labsys™TG-DTA16 (SETARAM) thermal analyzer was used to investigate the thermal property by the differential scanning calorimetric (DSC) analysis (the DSC was calibrated with Al_2O_3). About 15 mg of the $PbGa_4S_7$ sample was placed in a silica tube (5 mm o.d. × 3 mm i.d.) and subsequently sealed under a high vacuum. The heating and the cooling rates were both 10 K /min.

UV−vis−NIR Diffuse Reflectance Spectroscopy.

A Cary 5000 UV-vis-NIR spectrophotometer with a diffuse reflectance accessory was used to measure the spectrum of $PbGa_4S_7$ and $BaSO_4$ as a reference in the range 250 nm (5.0 eV) to 2500 nm (0.5 eV).

SHG Measurement.

The optical SHG response of $PbGa_4S_7$ was measured by means of the Kurtz–Perry method.[48] The fundamental light is the 2.09 μm light generated with a Q-switched Ho: Tm: Cr: YAG laser. About 300 mg $PbGa_4S_7$ crystals were hand-picked and ground to powder with the particle size of 105–150 μm for the measurement. Microcrystalline $AgGaS_2$ of a similar particle size served as a reference. The $AgGaS_2$ sample was homemade via reaction among the elements at high-temperature and its purity and quality was verified by the powder X-ray diffraction data.

Computational methods

The first-principles calculations at the atomic level for the $PbGa_4S_7$ crystal were

Journal of Materials Chemistry C Accepted Manuscript

performed by the plane-wave pseudopotential method[49] implemented in the CASTEP program[50] based on density functional theory (DFT) [51]. The exchange-correlation (XC) functionals was described by the local density approximation (LDA) [52]. The ion-electron interactions were modeled by the ultrasoft pseudopotentials[53] for all constituent elements. In this model, Pb $5d^{10}6s^26p^2$, Ga $3d^{10}4s^24p^1$, and S $3s^23p^4$ are treated as the valence electrons, respectively. The kinetic energy cutoff of 500 eV and Monkhorst-Pack *k*-point meshes[54] spanning less than 0.04/Å^3 in the Brillouin zone were chosen to ensure the sufficient accuracy of the present purposes.

Results and discussion

Synthesis.

The sulfide $PbGa_4S_7$ has been obtained from Bi_2S_3 flux for the first time. Although the synthesis of metal chalcogenides from Bi_2Q_3 flux is not common, the preparation of $PbGa_4S_7$ from Bi_2S_3 flux might open a way to further synthetic exploration of metal chalcogenides. We also made efforts to synthesize other new compounds in Pb-Ga-Q (Q = S, Se, Te) system. Unfortunately, the suspected $PbGa_6Q_{10}$ (Q = S, Se) and $PbGa_4Se_7$ were still of poor quality after many trials. Thus, we only report the study on $PbGa_4S_7$ here.

Crystal Structure.

Single crystal X-ray diffraction revealed that $PbGa_4S_7$ adopts the $BaGa_4Se_7$-type structure (Fig. 2 and Table 1), crystallizing in space group *Pc* of the monoclinic

Journal of Materials Chemistry C Accepted Manuscript

system with a = 7.281(1) Å, b = 6.339(1) Å, c = 12.385(3) Å, β = 105.97(3) °, and Z = 2. In the asymmetric unit, there are four crystallographically distinguished Ga atoms, one Pb atom, and seven S atoms. They are all at Wyckoff sites 2a with occupancy of 100%.

As shown in Fig. 2(a), the Ga atoms are coordinated by four S atoms in distorted tetrahedra with Ga–S bond length ranges from 2.222(3) to 2.333(2) Å (Table 2). Such a coordination environment of Ga atoms is often seen in similar chalcogenides, such as $BaGa_4S_7$ (2.228(13) to 2.338(17) Å)[17] and $BaGa_2GeS_6$ (2.246 to 2.264 Å).[20] The calculated bond valence sums (BVS)[56] values are 2.943, 2.882, 2.955, and 2.876 for Ga1, Ga2, Ga3, and Ga4 respectively, all close to the expected value of 3.000. Simultaneously, as demonstrated in the [Ga3S_4] tetrahedra (Fig. 2(a)), the Ga3–S6 distance (2.326(2) Å) is obviously longer than the other three (2.279(3) Å for Ga3–S1, 2.264(3) Å for Ga3–S3, and 2.237(2) Å for Ga3–S7) and all these Ga3–S6 bonds are aligned almost parallel to each other. Similar arrangements also exist in the [Ga1S_4], [Ga2S_4], and [Ga4S_4] tetrahedra, which give rise to the noncentrosymmetric and polar structure in this compound. Furthermore, the Pb atoms are bonded to five S atoms forming [PbS_5] distorted quadrangular pyramids with S1 atom at the apex, proving the existence of the stereochemically active lone-pair electrons on Pb^{2+}. The Pb–S bond distances vary from 2.742(3) to 3.533(3) Å, which are comparable to those observed in related compounds, such as $Pb_4Ga_4GeS_{12}$ (2.827(5) to 3.375(4) Å),[20] and PbU_2S_5 (2.786(16) to 3.103 (16) Å),[57] and the calculated BVS[55] value is 1.697, close to the expected value of 2.000.

Journal of Materials Chemistry C Accepted Manuscript

The structure of $PbGa_4S_7$ is illustrated in Fig. 2. The [GaS_4] tetrahedra connect with each other by corner sharing to form a tetrameric building block described as [Ga_4S_{11}] group (Fig. 2(b)). The [Ga_4S_{11}] groups are then connected by S2, S4 and S6 atoms to form a 2D Ga_4S_{11}-layer (Fig. 2(b)) lying parallel to the *ab* plane, which is further connected by S6 atoms along the *c* axis. Thus the structure of $PbGa_4S_7$ may be viewed as the 3D network (Fig. 2(c)) formed by the stack of 2D Ga_4S_{11}-layers (Fig. 2(b)) along the *c* axis with [PbS_5] distorted quadrangular pyramids locating in the cavities.

Although $PbGa_4S_7$ possesses the same stoichiometry as the previously reported $BaGa_4S_7$ compound, It crystallize in a different space group from $BaGa_4S_7$ ($Pmn2_1$). On one hand, they have some features in common: in both, the [GaS_4] tetrahedra share corners to form the 3D framework. However, the [GaS_4] tetrahedra are a little more distorted in $PbGa_4S_7$ than in $BaGa_4S_7$. Furthermore, the coordination preferences of Ba and Pb atoms are obviously different. In $PbGa_4S_7$, the Pb atom is covalently coordinated to a distorted quadrangular pyramid of five S atoms due to the steorechemical activity of lone pair electrons, whereas in $BaGa_4S_7$, the Ba atom is mostly ionic in character and centered by twelve S atoms forming a more "spherical" geometry for Ba. It means that, the interaction between two kinds of NCS groups, namely the [GaS_4] tetrahedra and the SOJT distorted cations, which might be beneficial for the NLO properties, exists in $PbGa_4S_7$, but not in $BaGa_4S_7$. In view of the space group and the atomic coordinates, $PbGa_4S_7$ may be classified into the $BaGa_4Se_7$ structure type (space group *Pc*). Still, the different coordination preferences

Journal of Materials Chemistry C Accepted Manuscript

between Ba and Pb are manifest in the two compounds, as the Ba atom in $BaGa_4Se_7$ is coordinated to eight Se atoms ranging from 3.429(2) to 3.861(2) Å, in contrast to the distorted quadrangular pyramidal environment of Pb with Pb–S bond distances varying from 2.742(3) to 3.533(3) Å in $PbGa_4S_7$.

Thermal Analysis.

The DSC curve of this compound is shown in Fig. 3. It is evident that $PbGa_4S_7$ has an endothermic peak at 1140 K, and an exothermic peak at 973 K. However, the PXRD pattern of the material after melting (Fig. 1) proves that the phase formed during cooling cycle is not $PbGa_4S_7$. Unfortunately, the exact structure of this after-cooling phase is not obtained yet. Still, this result indicates that $PbGa_4S_7$ melts incongruently.

Experimental Band Gap.

The optical diffuse reflectance method was used for the determination of the band gap. The optical band gap of sample can be determined by the following equation (1):[58,59]

$$(\alpha h\upsilon)^n = A(h\upsilon - E_g) \quad (1)$$

Where A is the absorption constant, h is Planck's constant, υ is the light frequency, E_g is the optical band gap, n is a constant exponent that determines the type of optical transitions. n equals to 1/2 and 2 for indirect and direct allowed transitions, respectively. α is absorption coefficient and is proportional to F(R). Based on the UV-Vis-NIR diffuse-reflectance spectrum, absorption (F(R)) data are calculated from the following Kubelka–Munk function (2):[60,61]

Journal of Materials Chemistry C Accepted Manuscript

$$F(R)=\frac{K}{S}=\frac{(1-R)^2}{2R} \quad (2)$$

where R is the reflectance, K is the absorption, and S is the scattering.

To determine the band gap being direct or indirect, the plots of $(F(R)hv)^2$ and $(F(R)hv)^{1/2}$ versus hv were performed according to Tauc method[62], shown in Fig. 4. The band gap obtained from the plots of $(F(R)hv)^2$ versus hv are much more consistent with the color of the compound. As a consequence, the compound possesses a direct band gap of 3.08 eV for $PbGa_4S_7$. Band gap has great influence on the laser damage threshold of IR NLO materials. Materials with large band gaps tend to have high laser damage thresholds. In comparison with the two related Ba compounds, namely $BaGa_4S_7$ and $BaGa_4Se_7$, both of which were reported to exhibit much higher laser damage thresholds than the traditional $AgGaQ_2$ (Q=S, Se) material, the band gap of $PbGa_4S_7$ lies in between those of $BaGa_4Se_7$ (2.64 eV) and $BaGa_4S_7$ (3.4 eV). Such a large band gap is a valuable property for achieving high laser damage threshold for $PbGa_4S_7$. Besides, the large band gap may allow the conventional 1 μm (Nd:YAG) or 1.55 μm (Yb:YAG) laser pumping without the two-photon absorption problem, which has plagued the benchmark IR NLO crystal $ZnGeP_2$.[63]

SHG Measurement.

As shown in Fig. 5, the powder SHG signal intensity of $PbGa_4S_7$ is ~1.2 times that of the commercial $AgGaS_2$ at a particle size of 105~150 μm, larger than that of $BaGa_4S_7$ (~ $AgGaS_2$).

In this structure, there are two kinds of microscopic NLO-active building blocks,

Journal of Materials Chemistry C Accepted Manuscript

namely the [PbS_5] and [GaS_4] units in the structure. The overall polar arrangement of the [GaS_4] units, as discussed in the structure part, is beneficial for generating large NLO responses. But the macroscopic arrangement of the [PbS_5] distorted quadrangular pyramid is a bit complicated. Fig. 6 illustrates the overall arrangement of the [PbS_5] distorted quadrangular pyramids themselves: although the [PbS_5] distorted quadrangular pyramids have the same orientation in the layers parallel to the *ac* plane, which would be conducive for enhancing the NLO response, these [PbS_5] distorted quadrangular pyramids are almost antiparallel in adjacent layers along the *b* axis, which is unfavorable for generating large NLO response. That is, the stereochemically active lone-pairR electrons on Pb^{2+} do not contribute significantly to the overall NLO response. It can be concluded that the [GaS_4] tetrahedra are still the dominant origin of the NLO response of $PbGa_4S_7$ and the contribution from [PbS_5] distorted quadrangular pyramid is of less importance. As a consequence, $PbGa_4S_7$ exhibits NLO response only a little larger than $BaGa_4S_7$.

Theoretical Results.

The electronic band structure of $PbGa_4S_7$ crystal in the unit cell is plotted along the symmetry lines in Fig. 7(a). The corresponding partial density of states (PDOS) projected on the constitutional atoms is plotted in Fig. 7(b). It is found that $PbGa_4S_7$ is a direct gap crystal, which agrees with experimental result, and its calculated value is 2.55 eV, slightly smaller than the experimental value (~ 3.08 eV) because the DFT calculations with the exchange-correlation (XC) functional of LDA always

Journal of Materials Chemistry C Accepted Manuscript

underestimate the band gap of a crystal. Note that the top of the valence band (VB) is mainly occupied by the *p* orbitals of Ga (4p) and S (3p), and slightly composed of the *s* orbitals of Ga (4s) and Pb (6s) at about –5 eV. The bottom of conduction band (CB) is mainly contributed by the orbitals of Pb (6p), Ga (4s) (4p) and S (3p). Namely, the states on both sides of the band gap are mainly composed of the orbitals from the $[GaS_4]^{5-}$ groups and secondarily from the $[PbS_5]^{8-}$ groups. Considering the optical response of a crystal in the visible-IR region originates mainly from the electronic transitions between the VB and CB states close to the band gap[64], the $[GaS_4]^{5-}$ and $[PbS_5]^{8-}$ anionic units mainly determine the optical properties of the IR $PbGa_4S_7$ crystal. In contrast, earlier study on the related $BaGa_4Se_7$ indicates that a large hybridization between Ga 4s (and 4p) and Se 4p orbitals around the Fermi Level and the $[Ga_4Se_7]^{2-}$ anionic framework determines the energy band gap of $BaGa_4Se_7$. It can be seen that Pb-containing compounds are distinct from Ba-containing compounds in view of the crystal structure, physical properties and electronic structure, which should result from the stereochemically active lone-pairR electrons and the more covalent nature of the Pb–Q bonding.

Furthermore, based on the obtained electronic structure, the SHG coefficients of $PbGa_4S_7$ crystal are computed by the scissors-corrected LDA method[65,66], including d_{11}=10.12 pm/V, d_{15}= –0.73 pm/V, d_{12}=4.35 pm/V, d_{13}= –11.91 pm/V, d_{24}=7.35 pm/V, d_{33}= –14.01 pm/V. The maximum is comparable to that of $AgGaS_2$ (d_{33}=13.7 pm/V), which is in a good accordance with experimental measurements.

Journal of Materials Chemistry C Accepted Manuscript

Conclusions

A new wide-gap IR NLO chalcogenide $PbGa_4S_7$ was obtained from Bi_2S_3 flux for the first time in Pb-Ga-Q system. Its structure is constructed by corner sharing [Ga_4S_{11}] groups with [PbS_5] distorted quadrangular pyramids residing in the cavities. The compound exhibits a large NLO response that is ~1.2 times that of the benchmark $AgGaS_2$ at a laser radiation of 2.09 μm. The NLO response mainly originates from [GaS_4] tetrahedra in the polar arrangement with secondary contribution from the stereochemically active lone-pair electrons on Pb^{2+}. The compound possess a wide band gap of 3.08 (2) eV, which is very beneficial for increasing the laser damage threshold and avoiding the two-photon absorption problem of conventional 1~2 μm pumping laser sources. The DSC analysis indicates that the compound is thermally stable up to 1140 K and the electronic structure calculation demonstrates that the band gap is mainly determined by the orbitals from the [GaS_4] groups and secondarily from the [PbS_5] groups. Such a compound may arouse further interest in exploring new IR NLO materials with Pb or other systems with lone pair electrons.

Acknowledgments

This research was supported by the National Natural Science Foundation of China (No.s 91122034, 51472251, and 21271178).

Journal of Materials Chemistry C Accepted Manuscript

References

1 W. Chen, G. Mouret, D. Boucher and F. K. Tittel, *Appl. Phys. B: Laser Opt.*, 2001, **72**, 873.

2 J. H. Liao, G. M. Marking, K. F. Hsu, Y. Matsushita, M. D. Ewbank, R. Borwick, P. Cunningham, M. J. Rosker and M. G. Kanatzidis, *J. Am. Chem. Soc.*, 2003, **125**, 9484.

3 S. Banerjee, C. D. Malliakas, J. I. Jang, J. B. Ketterson and M. G. Kanatzidis, *J. Am. Chem. Soc.*, 2008, **130**, 12270.

4 T. K. Bera, J. I. Jang, J. B. Ketterson and M. G. Kanatzidis, *J. Am. Chem. Soc.*, 2009, **131**, 75.

5 D. M. Burland, R. D. Miller and C. A. Walsh, *Chem. Rev.*, 1994, **94**, 31.

6 G. D. Boyd, H. Kasper and J. H. Mcfee, *IEEE J. Quantum Electron.*, 1971, QE7, **12**, 563.

7 A. Harasaki and K. J. Kato, *J. Appl. Phys.*, 1997, **36**, 700.

8 B. Tell and H. M. Kasper, *Phys. Rev. B*, 1971, **4**, 4455.

9 G. Airoldi, P. Beucherie and C. Rinaldi, *J. Cryst. Growth*, 1977, **38**, 239.

10 G. D. Boyd, E. Buehler and F. G. Storz, *Appl. Phys. Lett.*, 1971, **18**, 301.

11 B. W. Rudyk, S. S. Stoyko, A. O. Oliynyk and A. Mar, *J. Solid State Chem.*, 2014, **210**, 79.

12 Y. Xie, H. J. Chen, A. M. Li, X. L. Zhu, L. Zhang, M. S. Qin, Y. M. Wang, Y. F. Liu and F. Q. Huang, *J. Mater. Chem. A*, 2014, **2**, 13237.

13 G. N. Oh, E. S. Choi and J. A. Ibers, *Inorg. Chem.*, 2012, **51**, 4224.

Journal of Materials Chemistry C Accepted Manuscript

14 A. Mesbah, C. D. Malliakas, S. Lebegue, A. A. Sarjeant, W. Stojko, L. A. Koscielski and J. A. Ibers, *Inorg. Chem.*, 2014, **53**, 2899.

15 B. X. Li, Y. Wei, C. H. Huang, F. J. Zhuang, G. Zhang and G. C. Guo, *Spectrosc. Spectr. Anal.*, 2014, **34**, 6.

16 I. Chung and M. G. Kanatzidis, *Chem. Mater.*, 2014, **26**, 849.

17 X. S. Lin, G. Zhang and N. Ye, *Cryst. Growth & Des.*, 2009, **9**, 1186.

18 J. Y. Yao, D. J. Mei, L. Bai, Z. S. Lin, W. L. Yin, P. Z. Fu and Y. C. Wu, *Inorg. Chem.*, 2010, **49**, 9212.

19 W. L. Yin, K. Feng, W. Y. Hao, J. Y. Yao and Y. C. Wu, *Inorg. Chem.*, 2012, **51**, 5839.

20 W. L. Yin, K. Feng, R. He, D. J. Mei, Z. S. Lin, J. Y. Yao and Y. C. Wu, *Dalton Trans.*, 2012, **41**, 5653.

21 Y. K. Chen, M. C. Chen, L. J. Zhou, L. Chen and L. M. Wu, *Inorg. Chem.*, 2013, **52**, 8334.

22 M. C. Chen, L. M. Wu, H. Lin, L. J. Zhou and L. Chen, *J. Am. Chem. Soc.*, 2012, **134**, 6058.

23 Z. Z. Luo, C. S. Lin, H. H. Cui, W. L. Zhang, H. Zhang, Z. Z. He and W. D. Cheng, *Chem. Mater.*, 2014, **26**, 2743.

24 S. Banerjee, C. D. Malliakas, J. I. Jang, J. B. Ketterson and M. G. Kanatzidis, *J. Am. Chem. Soc.*, 2008,**130**, 12270.

25 T. K. Bera, J. I. Jang, J. H. Song, C. D. Malliakas, A. J. Freeman, J. B. Ketterson, and M. G. Kanatzidis, *J. Am. Chem. Soc.*, 2010, **132**, 3484.

Journal of Materials Chemistry C Accepted Manuscript

26 T. K. Bera, J. I. Jang, J. B. Ketterson and M. G. Kanatzidis, *J. Am. Chem. Soc.*, 2009, **131**, 75.

27 P.S. Halasyamani and K.R. Poeppelmeier, *Chem. Mater.*, 1998, **10**, 2753.

28 P. S. Halasyamani, *Chem. Mater.*, 2004, **16**, 3586.

29 P.S. Halasyamani, *Chem. Soc. Rev.*, 2006, **35**, 717

30 K. M. Ok, P. S. Halasyamani, D. Casanova, M. Llunell, P. Alomancy and S. Alvarez, *Chem. Mater.*, 2006, **18**, 3176.

31 W. L. Zhang, W. D. Cheng, H. Zhang, L. Geng, C. S. Lin and Z. Z. He, *J. Am. Chem. Soc.*, 2010, **132**, 1508.

32 F. Kong, S. P. Huang, Z. M. Sun, J. G. Mao and W. D. Cheng, *J. Am. Chem. Soc.*, 2006, **128**, 7750.

33 H. W. Yu, S. L. Pan, H. P. Wu, W. W. Zhao, F. F. Zhang, H. Y. Li and Z. H. Yang, *J. Mater. Chem.*, 2012, **22**, 2105.

34 H. Y. Li, H. P. Wu, X. Su, H. W. Yu, S. L. Pan, Z. H. Yang, Y. Lu, J. Han and K. R. Poeppelmeier, *J. Mater. Chem. C*, 2014, **2**, 1704.

35 H. Y. Chang, S. H. Kim, P. S. Halasyamani and K. M Ok, *J. Am. Chem. Soc.*, 2009, **131**, 2426.

36 W. L. Zhang, W. D. Cheng, H. Zhang, L. Geng, C. S. Lin and Z. Z. He, *J. Am. Chem. Soc.*, 2010, **132**, 1508.

37 C.F. Sun, C. L. Hu, X. Xu, J. B. Ling, T. Hu, F. Kong, X. X. Long and J. G. Mao, *J. Am. Chem. Soc.*, 2009, **131**, 9486.

Journal of Materials Chemistry C Accepted Manuscript

38 B. G. Tagiev, O. B. Tagiev, R. B. Dzhabbarov and N. N. Musaeva, *Inorg. Mater.*, 1999, **35**, 24.

39 A. Mazurier, S. Jaulmes and M. Guittard, *Acta Crystallogr. B*, 1980, **B36**, 1990.

40 L. Kienle and H. J. Deiseroth, *Z. Kristallogr.*, 1998, **213**, 569.

41 H. Kalpen, W. Honle, M. Somer, U. Schwarz, K. Peters, H. G. von Schnering and R. Blachnik, *Z. Anorg. Allg. Chem.*, 1998, **624**, 1137.

42 C. M. Thompson, K. Kovnir, S. Eveland, M. J. Herring and M. Shatruk, *Chem. Commun.*, 2011, **47**, 5563.

43 W. A. Phelan, G. V. Nguyen, J. K. Wang, G. T. McCandless, E. Morosan, J. F. DiTusa and J. Y. Chan, *Inorg. Chem.*, 2012, **51**, 11412.

44 J. J. Lu, T. S. Mo, K. J. Gan, J. F. Chou and M. K. Lee, *J. Supercon. Nov. Magn.*, 2011, **24**, 1991.

45 M. A. Measson, H. Muranaka, T. Kawai, Y. Ota, K. Sugiyama, M. Hagiwara, K. Kindo, T. Takeuchi, K. Shimizu, F. Honda, R. Settai and Y. Onuki, *J. Phys. Soc. Jpn.*, 2009, **78**, 12.

46 CrystalClear. Rigaku Corporation: Tokyo, Japan, 2008.

47 G. M. Sheldrick, *Acta Crystallogr. A*, 2008, **64**, 112.

48 S. K. Kurtz and T. T. Perry, *J. Appl. Phys.*, 1968, **39**, 3798.

49 M. C. Payne, M. P. Teter, D. C. Allan, T. A. Arias and J. D. Joannopoulos, *Rev. Mod. Phys.*, 1992, **64**, 1045.

50 S. J. Clark, M. D. Segall, C. J. Pickard, P. J. Hasnip, M. J. Probert, K. Refson and M. C. Payne, *Z. Kristallogr.*, 2005, **220**, 567.

Journal of Materials Chemistry C Accepted Manuscript

51 W. Kohn, *Rev. Mod. Phys.*, 1999, **71**, 1253.

52 D. M. Ceperley and B. J. Alder, *Phys. Rev. Lett.*, 1980, **45**, 566.

53 J. S. Lin, A. Qteish, M. C. Payne and V. Heine, *Phys. Rev. B*, 1993, **47**, 4174.

54 H. J. Monkhorst and J. D. Pack, *Phys. Rev. B*, 1976, **13**, 5188.

55 B. G. Pfrommer, M. Cote, S. G. Louie and M. L. Cohen, *J. Comput. Phys.*, 1997, **131**, 233C.

56 I. D. Brown and D. Altermatt, *Acta Crystallogr., Sect. B: Struct. Sci.* 1985, **41**, 244.

57 J. Prakash, M. S. Tarasenko, A. Mesbah, S. Lebegue, C. D. Malliakas and J. A. Ibers, *Inorg. Chem.*, 2014, **53**, 11626.

58 C. Aydın, M. Benhaliliba, A. A. Al-Ghamdi, Z. H. Gafer, F. El-Tantawy, F. Yakuphanoglu, *J. Electroceram.*, 2013, **31**, 265.

59 F. Yakuphanoglu, S. Ilican, M. Caglar and Y. Caglar, J. Optoelectron. *Adv. Mater.*, 2007, **9**, 2180.

60 C. Aydın, M. S. Abd El-sadek, K. Zheng, I. S. Yahia and F. Yakuphanoglu, *Opt. Laser Technol.*, 2013, **48**, 447.

61 E. L. Simmons, *Appl. Opt.*, 1975, **14**, 1380.

62 J. Tauc, R. Grigorovici and A. Vancu, *Phys. Stat. Sol. (b)*, 1966, **15**, 627.

63 P. G. Schunemann, *AIP Conf. Proc.*, 2007, **916**, 541.

64 M. H. Lee, C. H. Yang and J. H. Jan, *Phys. Rev. B*, 2004, **70**, 5110.

65 C. S. Wang and B. M. Klein, *Phys. Rev. B*, 1981, **24**, 3393.

66 R. W. Godby, M. Schluter and L. J. Sham, *Phys. Rev. B*, 1988, **37**, 10159.

Journal of Materials Chemistry C Accepted Manuscript

Fig. Captions

Fig. 1. Experimental (blue and red) and simulated (black) X-ray powder diffraction data of $PbGa_4S_7$ (the tiny extra peak at around 24° may come from very tiny amount of unknown impurity).

Fig. 2. (a) Coordination environments of all cations in $PbGa_4S_7$. Gray, Pb; blue, Ga and $[GaS_4]$ tetrahedra; yellow, S. (b) A single 2D Ga_4S_{11}-layer perpendicular to the *c* direction with a single $[Ga_4S_{11}]$ group marked by a red circle. (c) Crystal packing structure of $PbGa_4S_7$ viewed down the *b*-axis with the unit cell marked.

Fig. 3. The DSC pattern of $PbGa_4S_7$.

Fig. 4. Optical reflection spectrum of $PbGa_4S_7$: (a) the plot of $(F(R)hv)^2$ versus hv; (b) the plot of $(F(R)hv)^{1/2}$ versus hv.

Fig. 5. Oscilloscope traces of SHG signals for $PbGa_4S_7$ with $AgGaS_2$ as a reference at a particle size of 105~150 μm.

Fig. 6. Macroscopic packing of $[PbS_5]$ polyhedra in the structure.

Fig. 7. The band structure (a) and the total and partial density of states (DOS and PDOS, respectively) of $PbGa_4S_7$. Dashed line represents the Fermi energy (E_f).

Journal of Materials Chemistry C Accepted Manuscript

Table 1. Crystal data and structure refinement for $PbGa_4S_7$

	$PbGa_4S_7$
fw	710.49
T (K)	153
a (Å)	7.281(1)
b (Å)	6.339(1)
c (Å)	12.385(3)
β (deg)	105.97(3)
space group	*Pc*
V (Å^3)	549.6(2)
Z	2
ρ_c (g cm^{-3})	4.293
μ (mm^{-1})	26.210
$R(F)^a$	0.0298
$R_w(F_o^2)^b$	0.0589
Flack parameter	0.010(6)

$^aR(F) = \sum||F_o|-|F_c||/\sum|F_o|$ for $F_o^2 > 2\sigma(F_o^2)$. $^bR_w(F_o^2) = \{\sum[w(F_o^2 - F_c^2)^2] / \sum wF_o^4\}^{½}$ for all data. $w^{-1} = \sigma^2(F_o^2) + (zP)^2$, where $P = (\mathrm{Max}(F_o^2, 0) + 2\,F_c^2)/3$; $z = 0.09$.

Journal of Materials Chemistry C Accepted Manuscript

Table 2. Selected bond lengths (Å) for $PbGa_4S_7$

$PbGa_4S_7$		$PbGa_4S_7$	
Pb1–S1	2.742(3)	Ga2–S5	2.314(2)
Pb1–S2	3.023(3)	Ga2–S6	2.289(2)
Pb1–S3	2.771(3)	Ga3–S1	2.279(3)
Pb1–S4	3.070(3)	Ga3–S3	2.264(3)
Pb1–S7	3.533(3)	Ga3–S6	2.326(2)
Ga1–S4	2.245(3)	Ga3–S7	2.237(2)
Ga1–S5	2.325(2)	Ga4–S2	2.273(3)
Ga1–S6	2.326(2)	Ga4–S3	2.286(3)
Ga1–S7	2.222(3)	Ga4–S4	2.253(3)
Ga2–S1	2.283(3)	Ga4–S5	2.333(2)
Ga2–S2	2.253(3)		

Journal of Materials Chemistry C Accepted Manuscript

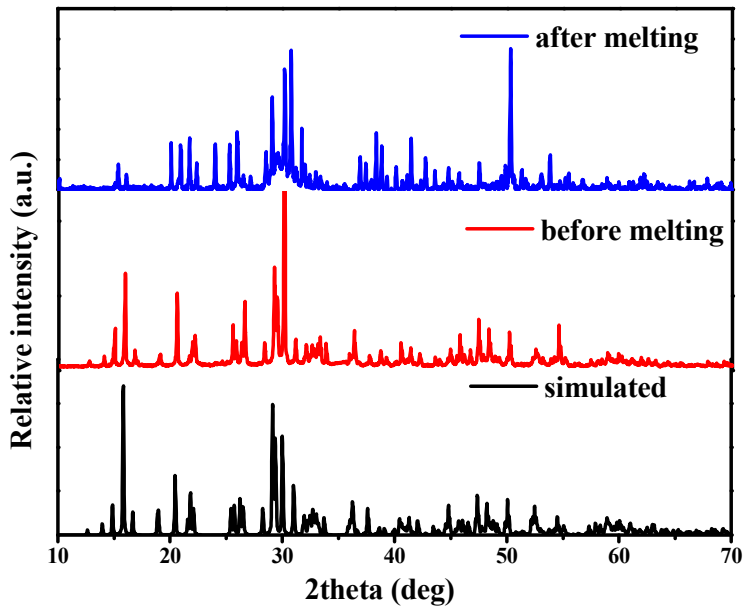

Fig. 1. Experimental (blue and red) and simulated (black) X-ray powder diffraction data of $PbGa_4S_7$.

Journal of Materials Chemistry C Accepted Manuscript

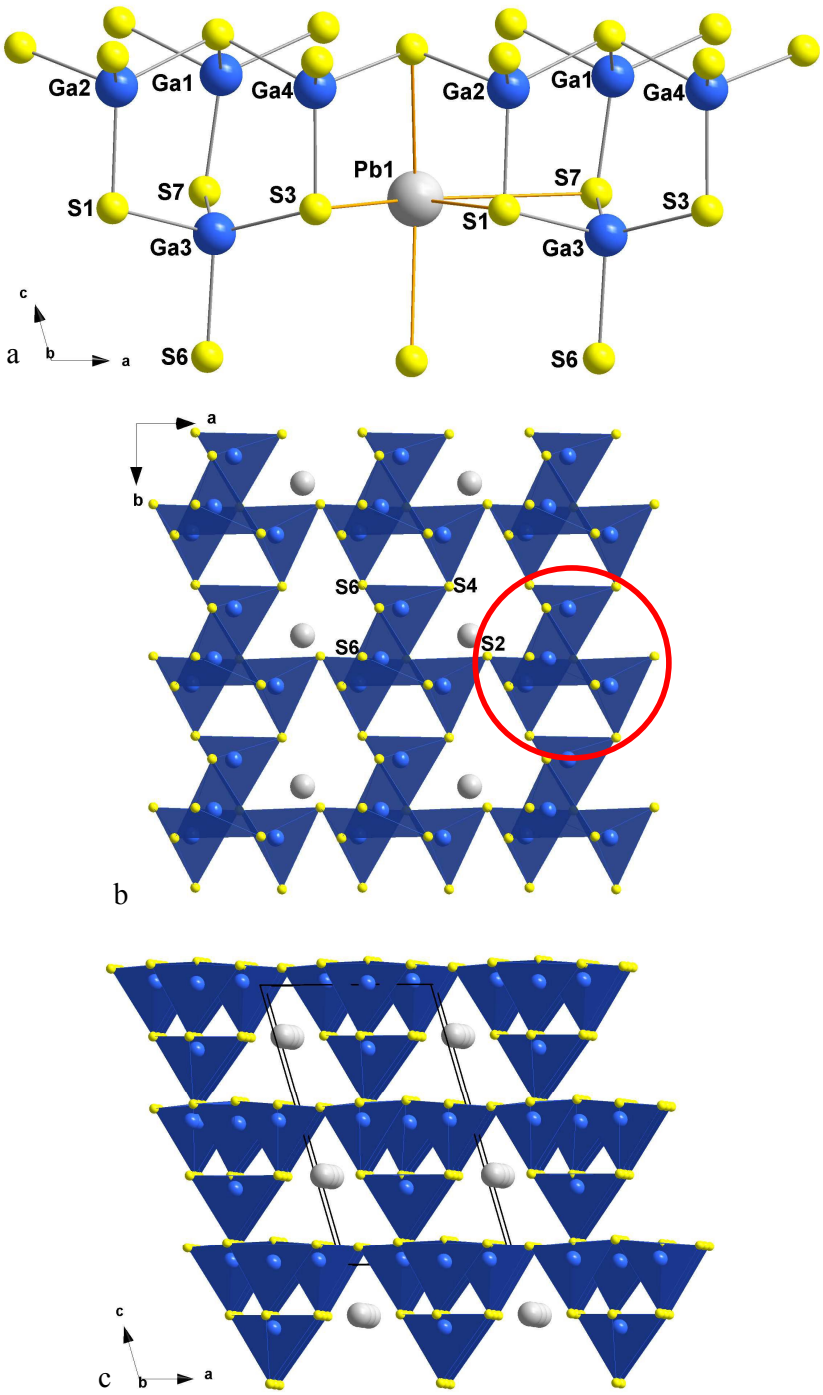

Fig. 2. (a) Coordination environments of all cations in $PbGa_4S_7$. Gray, Pb; blue, Ga and $[GaS_4]$ tetrahedra; yellow, S. (b) A single 2D Ga_4S_{11}-layer perpendicular to the c direction with a single $[Ga_4S_{11}]$ group marked by a red circle. (c) Crystal packing structure of $PbGa_4S_7$ viewed down the b-axis with the unit cell marked.

Journal of Materials Chemistry C Accepted Manuscript

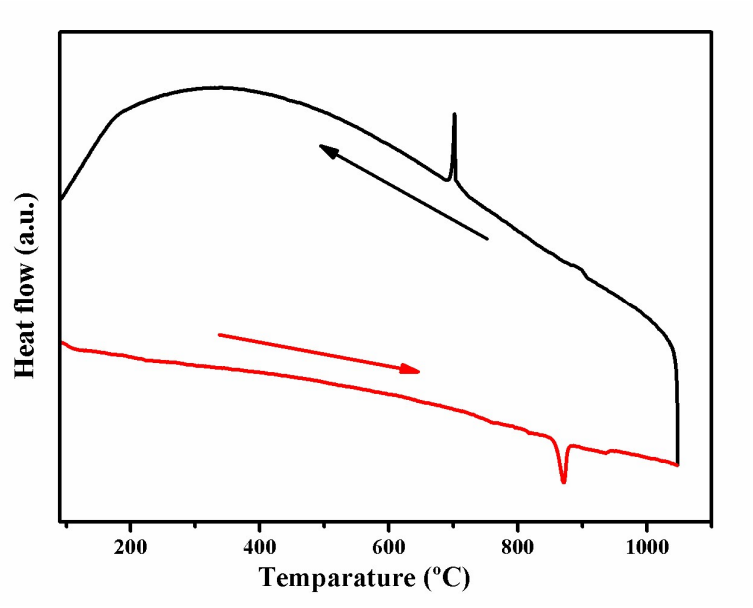

Fig. 3. The DSC patterns of $PbGa_4S_7$.

Journal of Materials Chemistry C Accepted Manuscript

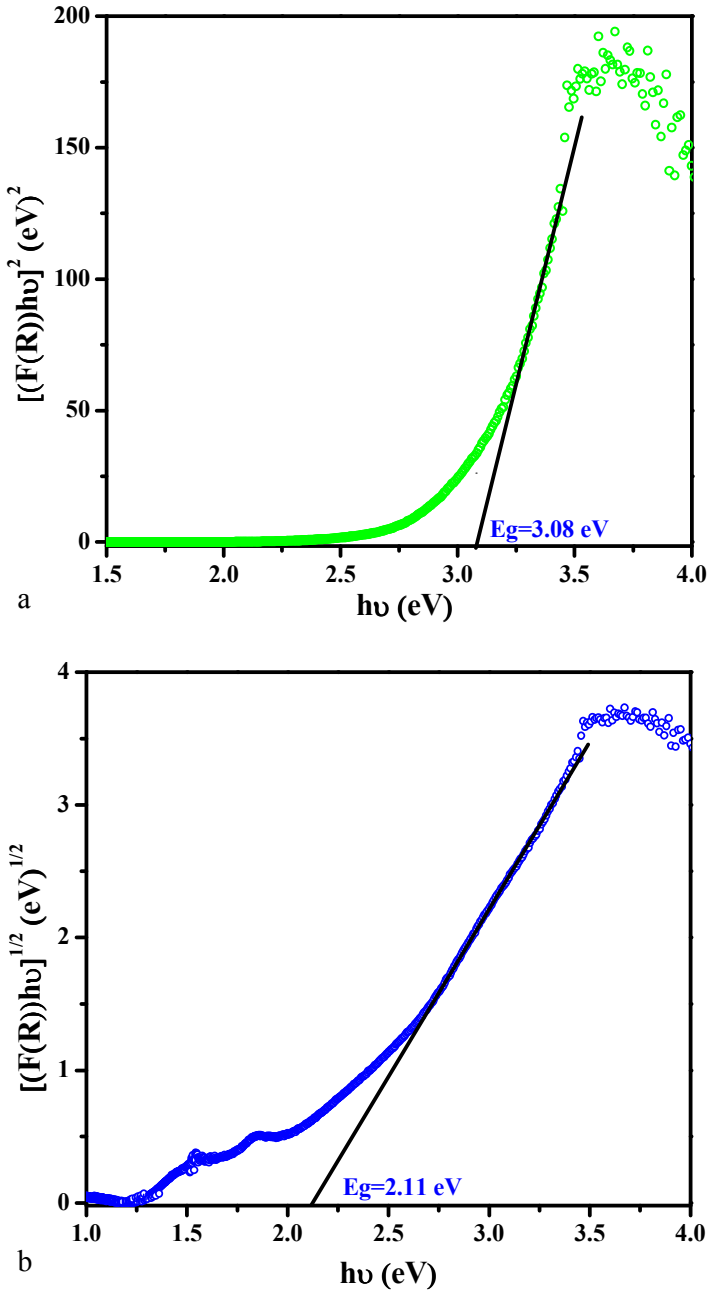

Fig. 4. Optical reflection spectrum of $PbGa_4S_7$: (a) the plot of $(F(R)hv)^2$ versus hv; (b) the plot of $(F(R)hv)^{1/2}$ versus hv.

Journal of Materials Chemistry C Accepted Manuscript

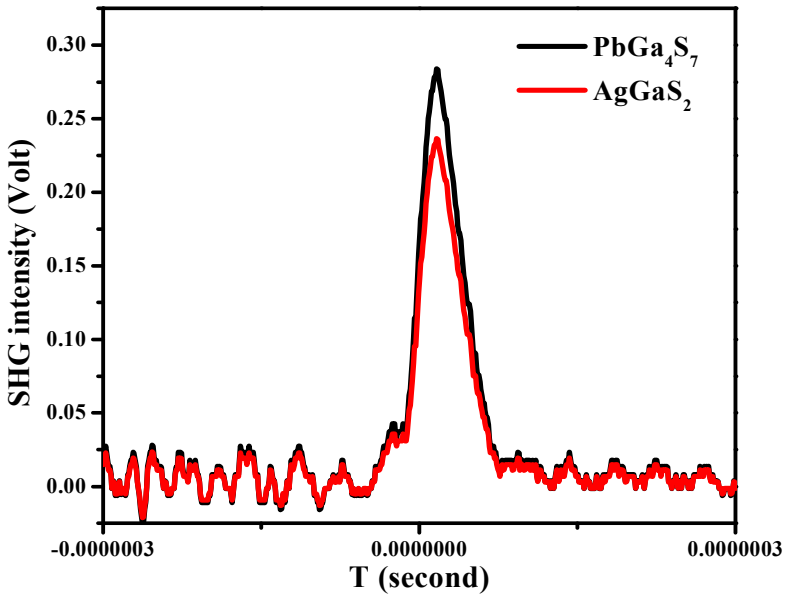

Fig. 5. Oscilloscope traces of SHG signals for $PbGa_4S_7$ with $AgGaS_2$ as a reference at a particle size of 105~150 μm.

Journal of Materials Chemistry C Accepted Manuscript

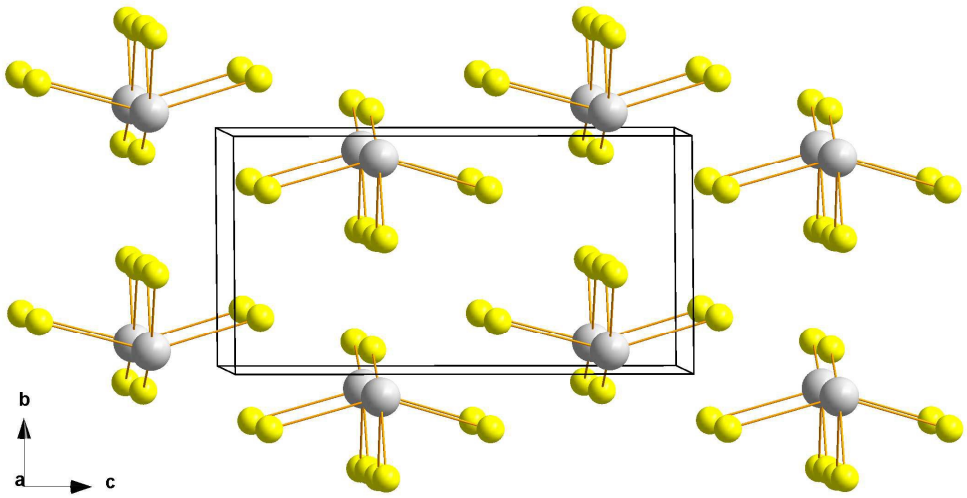

Fig. 6. Macroscopic packing of [PbS_5] polyhedra in the structure.

Journal of Materials Chemistry C Accepted Manuscript

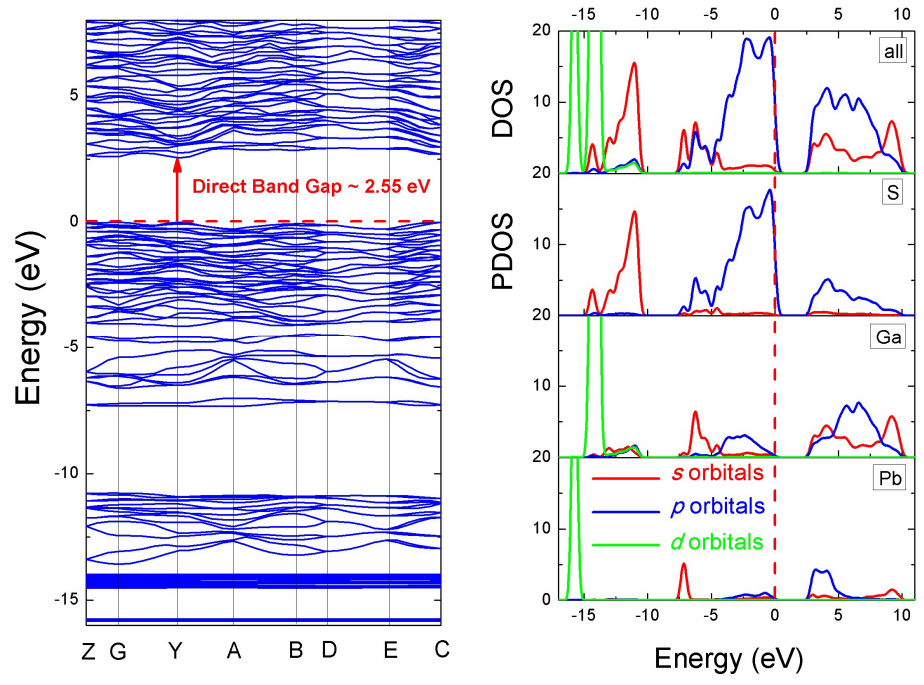

Fig. 7. The total and partial density of states (DOS and PDOS, respectively) of $PbGa_4S_7$. Dashed line represents the Fermi energy (E_f).

Journal of Materials Chemistry C Accepted Manuscript

Table of Contents Entry

$PbGa_4S_7$ possesses a large powder second harmonic generation response and a large direct band gap of 3.08 eV.

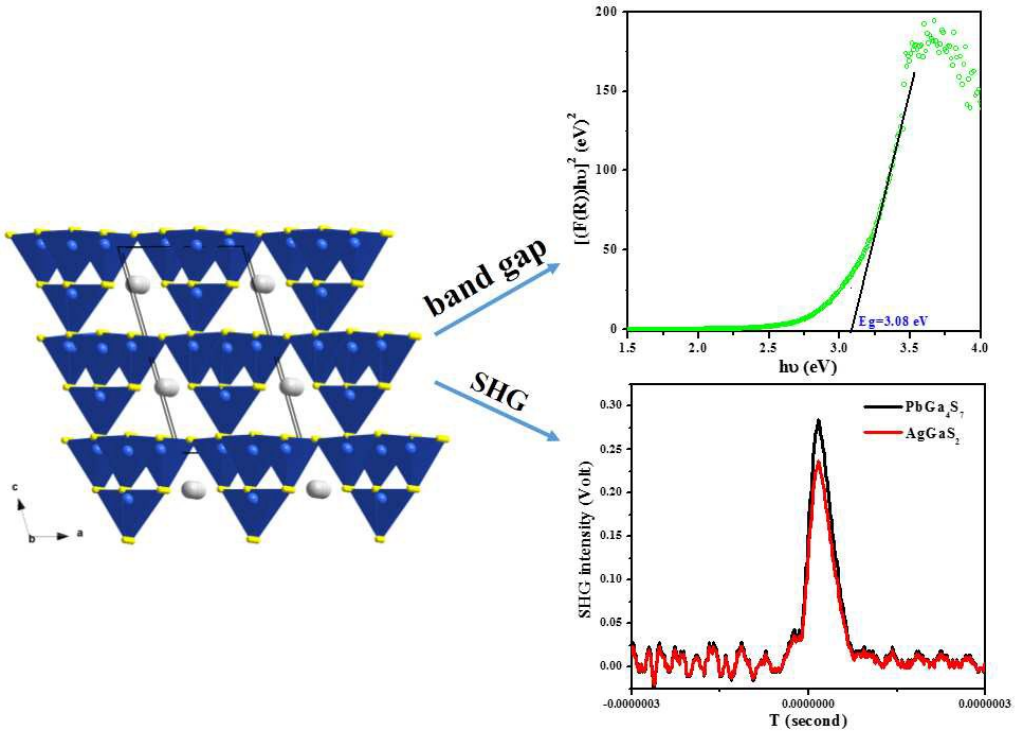

Journal of Materials Chemistry C Accepted Manuscript